Received: 31 March 2020 | Revised: 19 July 2020 | Accepted: 26 July 2020

DOI: 10.1002/jbm.a.37085

Society For Biomaterials

WILEY

ORIGINAL ARTICLE

Heparin/collagen surface coatings modulate the growth, secretome, and morphology of human mesenchymal stromal cell response to interferon-gamma

Said J. Cifuentes[1] | Priyanka Priyadarshani[2,3] | David A. Castilla-Casadiego[4] | Luke J. Mortensen[2,3] | Jorge Almodóvar[4] | Maribella Domenech[1,5]

[1]Bioengineering Graduate Program, University of Puerto Rico Mayaguez, Mayaguez, Puerto Rico

[2]Regenerative Bioscience Center, Rhodes Center for ADS, University of Georgia, Athens, Georgia

[3]School of Chemical, Materials and Biomedical Engineering, University of Georgia, Athens, Georgia

[4]Ralph E. Martin Department of Chemical Engineering, University of Arkansas, Fayetteville, Arkansas

[5]Department of Chemical Engineering, University of Puerto Rico Mayagüez, Mayagüez, Puerto Rico

Correspondence
Jorge Almodóvar, Ralph E. Martin Department of Chemical Engineering, University of Arkansas, 3202 Bell Engineering Center, Fayetteville, AR 72701, USA.
Email: jlalmodo@uark.edu

Maribella Domenech, Bioengineering Graduate Program, University of Puerto Rico Mayaguez Call Box 9000, Mayaguez, PR 00681-9000, USA.
Email: maribella.domenech@upr.edu

Funding information
Center for the Advancement of Wearable Technologies, National Science Foundation, Grant/Award Number: OIA-1849243; Engineering Center for Cell Manufacturing Technologies, National Science Foundation, Grant/Award Number: EEC-1648035; PUERTO RICO IDEA NETWORK OF BIOMEDICAL RESEARCH EXCELLENCE, National Institute of Health, Grant/Award Number: P20 GM103475-15

Abstract

The therapeutic potential of human mesenchymal stromal cells (h-MSC) is dependent on the viability and secretory capacity of cells both modulated by the culture environment. Our previous studies introduced heparin and collagen I (HEP/COL) alternating stacked layers as a potential substrate to enhance the secretion of immunosuppressive factors of h-MSCs. Herein, we examined the impact of HEP/COL multilayers on the growth, morphology, and secretome of bone marrow and adipose-derived h-MSCs. The physicochemical properties and stability of the HEP/COL coatings were confirmed at 0 and 30 days. Cell growth was examined using cell culture media supplemented with 2 and 10% serum for 5 days. Results showed that HEP/COL multilayers supported h-MSC growth in 2% serum at levels equivalent to 10% serum. COL and HEP as single component coatings had limited impact on cell growth. Senescent studies performed over three sequential passages showed that HEP/COL multilayers did not impair the replicative capacity of h-MSCs. Examination of 27 cytokines showed significant enhancements in eight factors, including intracellular indoleamine 2, 3-dioxygenase, on HEP/COL multilayers when stimulated with interferon-gamma (IFN-γ). Image-based analysis of cell micrographs showed that serum influences h-MSC morphology; however, HEP-ended multilayers generated distinct morphological changes in response to IFN-γ, suggesting an optical detectable assessment of h-MSCs immunosuppressive potency. This study supports HEP/COL multilayers as a culture substrate for undifferentiated h-MSCs cultured in reduced serum conditions.

KEYWORDS

collagen type I, heparin, human mesenchymal stromal cells, IDO, IFN-γ, layer-by-layer

1 | INTRODUCTION

Human mesenchymal stromal cells (h-MSCs) have great potential in the field of regenerative medicine based on their multilineage differentiation capability, self-renewal capacity, and their immunomodulatory potential observed in both in vitro and in vivo.[1,2] A considerable effort embodied in the more than 66 h-MSCs based investigational new drugs (IND) submitted since 2006[3] supports a

growing interest and clinical need for h-MSCs from different adult tissues to treat a variety of diseases.[4] As the field progresses toward refining the therapeutic applications of undifferentiated h-MSCs for the treatment of inflammatory disorders among which are multiple sclerosis[5] and type 1 diabetes,[6] the cell expansion methods and quality assessments will need to be optimized to fulfill the growing clinical demand and increase the affordability of such therapies.[4,7]

The cell expansion process has been identified as one of the steps that contribute to high production costs[8] and a key determinant of the therapeutic quality of cells.[9] The supplementation of growth factors to support cell growth and potency is one of the main drivers of cost at the early stages of cell production, representing about 30–40% of the cost of raw materials.[3,10] Several efforts have been performed to reduce costs associated with cell expansion at higher cell yields while maintaining potency. Yet these methods are either too expensive or not focused on the therapeutic application of undifferentiated h-MSCs. Some of the proposed strategies include optimized media formulations and stacks of multiple two-dimensional culture chambers, such as The Cell Factory (ThermoFisher Scientific, Waltham, MA) and CellStack/HyperStack (Corning, New York, NY). These 2D culture alternatives offer a substantial increase of around 36 fold in cell yield at a reduced spatial footprint, in comparison to traditional 2D methods,[11,12] but the high cost of these culture platforms does not provide a substantial cost reduction in the overall cell expansion process. Chemically defined media like STEMPRO® MSC SFM (Invitrogen, Carlsbad, CAUSA) have arisen to provide robust culture conditions for the expansion of h-MSCs, minimizing issues related to lot-to-lot variability and xenogeneic pathogens[13] associated with animal-derived media; however, this growth media requires a special coating (CELLstart™, Invitrogen, Carlsbad, CA) for cell anchoring, which makes this culture strategy about 10 times more expensive than standard serum-supplemented cultures. Moreover, the use of STEMPRO® MSC SFM has been reported to promote stromal cell fate toward the osteogenic lineage,[14] suggesting that this media formulation is better suited for bone tissue engineering applications using h-MSCs.[15] Another alternative for h-MSC expansion is the use of bioreactors that could enable the production of a high number of cells in an environment with well-controlled key parameters (e.g., oxygen, dissolved CO_2, metabolites concentration, and so forth).[16] Although these strategies offer a substantial benefit for generating high cell numbers, they do not necessarily maintain or improve the therapeutic potency of h-MSCs being generated. A decrease in cell potency will require a higher number of cells to achieve a therapeutic dosage,[17,18] thereby abrogating the benefit of high cell yields.

A relatively unexplored strategy for the expansion of undifferentiated h-MSCs is the use of surface coatings as cell culture interfaces for the stimulation of intrinsic cell signals and prolonged growth factor availability. Culture substrates made of natural and synthetic components mimetic of the extracellular matrix (ECM) have been shown to stimulate the growth and secretory capabilities of h-MSCs through both biochemical and biophysical signals.[19,20] For example, integrin-mediated cell binding has been shown to contribute to cell survival, while cell proteolytic remodeling enhances the interaction of ECM-sequestered growth factors with cell receptors.[21] ECM-derived biomolecules, such as heparin sulfate, can prolong growth factor availability by sequestering proteins and peptides secreted from cells or supplemented in the media, amplifying both the intrinsic and extrinsic growth stimulus, and thus diminishing the need for frequent growth factor supplementation.[22]

The deposition of thin polymeric layers is a low-cost strategy to generate surface coatings on culture surfaces. One approach to generate thin surface coatings of polymers on culture surfaces is the layer-by-layer (LbL) deposition method. This method consists of surface dipping multi-steps to generate polyelectrolyte stacked multilayers of oppositely charged materials. The LbL technique has been widely used as a strategy to study natural polymers to enhance cell adhesion, proliferative index, and differentiation capability using in vitro culture platforms.[23] Substrates generated by the LbL technique have been used for the immobilization of natural molecules without the need of high temperatures and nonaqueous solutions that affect molecules bioactivity.[24] Moreover, this technique offers the possibility to explore the combined effect of the deposited layers by they confirmed interdigitation as reported by Picart et al. among others.[25-27] LbL-produced substrates are generated via cycles of dipping, it can be adapted to 2D flat surfaces and suspended cultures, such as microcarriers.[28] Such versatility facilitates its transition to a scale-up system to complement current approaches in a bioreactor vessel.

In our previous work, we introduced the use of LbL multilayers composed of heparin and collagen I as a culture substrate for h-MSCs.[29] We showed that heparin and collagen I (HEP/COL) multilayers outperformed tissue culture plastic (TCP) in cell growth and secretion of four cytokines (IL-6, VEGF-A, FGF-2, and M-CSF) from bone marrow-derived MSCs (BMSCs) stimulated with interferon-gamma (IFN-γ) cultured in media supplemented with 20% serum.[29] In this study, we further examine the capacity of HEP/COL multilayers to support h-MSC culture. We examined the sequential deposition and stability of the HEP/COL multilayers at 0 and 30 days, and expanded our previous findings by examining its impact in the growth, morphology, senescence and secretome profile of 27 cytokines of h-MSC derived from both bone marrow and adipose tissues. Cell growth was compared among HEP/COL multilayers and single component surface coatings, and culture media supplemented with 10 or 2% serum. A computer-aided morphological assessment was performed to identify a correlation among h-MSCs morphological differences and their secretory potential.

2 | MATERIALS AND METHODS

2.1 | Surface deposition of HEP/COL multilayers

Lyophilized COL from bovine tendon (provided by Integra Lifesciences Holdings Corporation, Añasco, PR) and HEP sodium (PH3005, Celsus Laboratories, Cincinnati, OH) were used to construct multilayers on flat bottom tissue culture treated 96-well plates from NEST (701,001, ThermoFisher Scientific, Nashville, TN), following the

procedure as described by Castilla et al.[30] Briefly, polymers were dissolved at a concentration of 1.0 mg/ml in acetate buffer pH 5 (0.1 M sodium acetate anhydrous and 0.1 M acetic acid glacial dissolved in ultrapure water 18 MΩ-cm from tap producing RiOs™ and Milli-Q® water system). LbL technique was employed to construct polymeric multilayers of HEP/COL (ended either in HEP or COL). Briefly, the culture surface is charged by adding 200 μl of polyethyleneimine (PEI) at 1.0 mg/ml in acetate buffer (P3143, Sigma–Aldrich, St. Louis, MO) and incubated for 15 min. PEI established an anchoring surface for subsequent deposition of alternate layers of HEP and COL. Each polymer layer deposition consisted of 5 min incubation followed by a 3 min washing with acetate buffer (pH 5) until the desired number of alternating COL and HEP layers was reached. A final wash was performed using sterile Dulbecco's phosphate-buffered saline (DPBS) 1X and substrates were immediately sterilized inside the biosafety cabinet using UV light for 10 min. Stacked multilayers, with an even number of layers ended in COL, while those that have an odd number of layers ended in HEP, as shown in Figure 2b.

2.2 | Physicochemical characterization of HEP/COL multilayers

Multilayers of HEP/COL were fabricated over silicon substrates, following a procedure analogous to what was described in the previous section. An automated dipping machine nanoStrata StratoSequence VI (Tallahassee, Florida) was used to sequentially immerse silicon substrates in each polymeric solution until desired number of layers were deposited. Infrared Variable Angle Spectroscopic Ellipsometry (IR-VASE®-Mark II, J.A. Woollam Co., Inc. IR-VASE, Lincoln, Nebraska) was used to determine the thickness and chemistry of the HEP/COL multilayered substrates at 25°C as described by Castilla et al.[30] Characterization was performed at 0 and 30 days postfabrication after storage at room conditions, 22°C and 40% relative humidity. The identification of relevant functional groups for all samples was performed in a wavenumber range from 800–1700 cm^{-1} and the measurements by a deuterated triglycine sulfate (DTGS) detector with an angle of incidence of 70°, a spectral resolution of 16 cm^{-1}, 200 scans per cycle, 1 cycle, bandwidth of 0, minimum intensity ratio of 5, sample type as isotropic, zone average polarizer, and rotating compensator ellipsometry (RCE) analyzer on zone average analyzer. Multilayer thickness was measured using the IR-VASE® instrument and the WVASE32 software by a fitting procedure that produces ellipsometric models defined by optical constants (n, k) and film thickness from collected data.

A physical surface analysis was performed to determine the percentage of surface coverage as a function of deposited layers. Surface coverage of deposited multilayers was assessed after the sequential deposition of HEP and COL alternating layers on a silicon wafer. Data obtained were quantified using a KEYENCE 3D laser scanning confocal microscope VK-X series in laser confocal mode, at a magnification of ×50, superfine resolution, high precision quality and 0.1 μm pitch.

The increase on surface thickness during the sequential deposition of HEP/COL multilayers was assessed by surface plasmon resonance (SPR). SPR detection was performed using an MP-SPR Navi™ 210A VASA (Bio-Navis Ltd.) were alternated deposition of HEP and COL was carried out on a gold-coated sensor for MS-SPR (SPR102-AU, Bio-Navis Ltd.). All measurements were done on a standard PEEK Flow cell for MP-SPR Navi 210A VASA. The solutions were injected automatically (PEI, HEP, and COL) for 4 min injection and 5 min post wait after injection with buffer flow, the buffer was run for 10 min at 50 μl/min prior to the initiation of the automatic sequence, SPR angular scans (two wavelength mode) were recorded in a range from 60 to 78°. The temperature was kept at 25°C. The BioNavis Data Viewer software was used for data processing.

2.3 | MSC cultures

Adipose-derived stromal cells (ADSCs) from two donors (PT-5006, Lonza, Rochester, NY) and (MSC-022, lot 00097, RoosterBio®, Frederick, MD), and BMSCs from two donors (MSC-003, lot 00182 and lot 00114, from RoosterBio®) were used in this study. According to their product specification sheets, these cells conserved Adipogenic and Osteogenic potential, and were positive for CD90 and CD166 surface markers, and negative for CD34 and CD45. These h-MSCs were thawed and expanded to create a master cell banks in T175 CELLSTAR cell culture flasks (660,175, vwr™, Atlanta, GA) using either a Rooster Basal™-MSC (SU-005) media supplemented with Rooster Booster™-MSC (SU-003) for RoosterBio cells or MSCGM™ Mesenchymal Stem Cell Growth Medium BulletKit™(PT-3001, Lonza, Rochester, NY) for Lonza ADSCs. All cells were certified mycoplasma-free and kept inside a humidified incubator (37°C, 5% CO_2). Regular media changes were done every 3 days. Cells were harvested once confluence reached 75–80% after 7–8 days in culture using 0.25% trypsin ethylenediaminetetraacetic acid (EDTA) solution (59418C, Sigma–Aldrich, St. Louis, MO).

To identify the optimal number of multilayers for cell growth, ADSCs (PT-5006, Lonza) of passage 7 were cultured on TCP and the generated HEP/COL multilayers, with surface deposited layers ranging from 8 to 17 for a total of 5 days. Cells were kept in 5% CO_2 at 37°C while cultured in Dulbecco's Modified Eagle's Medium (DMEM)-high glucose (D5796), with 2% heat-inactivated fetal bovine serum (F6765), and 1% penicillin/streptomycin (P4333) from Sigma–Aldrich. RoosterBio h-MSCs (ADSCs MSC-022, and BMSCs MSC-003) were seeded on 96-well plates coated with either COL-ended (8-L) or HEP-ended multilayers (9-L). Cells were incubated in DMEM-high glucose supplemented with either 2 or 10% heat-inactivated fetal bovine serum (FBS), 1% penicillin/streptomycin, and 1% Gibco™ MEM Non-Essential Amino Acids Solution (12,084,947, ThermoFisher Scientific, Nashville, TN) and maintained at 5% CO_2 and 37°C for 5 days. Cells were used between passages 3 and 7 at a seeding density of 3500 cells/cm^2.

2.4 | Cell viability

PrestoBlue™ Cell Viability Reagent from Invitrogen (A13261, ThermoFisher Scientific, Nashville, TN) was used to measure the cell viability of h-MSCs at 5 days. A 20 min reagent incubation was followed

according to the vendor's protocol. Finally, viability was measured in a Tecan Infinite® 200 PRO plate reader in fluorescence mode (560 nm Ex. and 590 nm Em.), and data were summarized per cell line and culture conditions.

2.5 | Replicative senescence

Bone marrow (MSC-003, lot 00182) and adipose (MSC-022, lot 00097) h-MSCs (both from passage 3) were cultured on TCP, 8-L and 9-L in 12-well plates at a seeding density of 9000 cells/cm^2. Cells were cultured in DMEM supplemented with 1% pen-strep, 1% MEM non-essential amino acids and either 2 or 10% heat-inactivated FBS and maintained at 37°C and 5% CO_2. Cells were harvested with 0.25% trypsin EDTA solution and seeded in wells every 4 days using the same culture conditions. Cell senescence was examined at 4, 8, and 12 days using the Senescence β-Galactosidase Staining Kit (50–195-853, Fisher Scientific, Pittsburgh, PA) according to the manufacturer's protocol. Briefly, growth media was aspirated followed by a wash with 1 ml DPBS 1X for each culture well. Next, cells were fixed with 500 μl/well 1X Fixative Solution for 13 min, washed twice with DPBS 1X and incubated overnight using 500 μl/well of β-Galactosidase Staining Solution and maintained at 37°C in a non-CO_2 dry incubator. Cells were stained with the nuclear dye Hoechst 33342 (H3570, ThermoFisher Scientific, Nashville, TN). Brightfield and fluorescent images were taken at ×10 magnification using a KEYENCE BZ-X800 microscope. The percentage of β-galactosidase positive cells was determined by dividing the number of blue stained cells by the total number of cells obtained from fluorescent overlapping micrographs of nuclear stained DNA. A total of four images per well was used to compute the average percentage of β-galactosidase positive cells per well.

2.6 | Intracellular indoleamine 2, 3-dioxygenase assay

ADSCs and BMSCs were seeded as a monolayer at a density of 9000 cells/cm^2 on TCP, 8-L, and 9-L substrates in 6-well plates (3516, Fisher Scientific, Pittsburgh, PA). Cell aggregates were generated by seeding 18,000 cells/well in a low attachment round-bottom 96-well plate (4515, Fisher Scientific, Pittsburgh, PA). DMEM supplemented with 2% heat-inactivated FBS, 1% penicillin/streptomycin, 1% MEM non-essential amino acids solution, and ± 20 ng/ml of IFN-γ were used for cell culture. Culture supernatants and cell lysates were collected and stored at −80°C after 5 days in culture. To measure intracellular indoleamine 2, 3-dioxygenase (IDO) activity, cells were lysed and tested for N-formylkynurenine production (NFK) according to the Indoleamine 2, 3-Dioxygenase 1 (IDO1) Activity Assay Kit (K972-100, BioVision, Milpitas, CA) manufacturer's protocol. Cells were recovered from each substrate and spun to isolate pellets from each condition. Samples were lysed by adding 200 μl ice-cold IDO assay buffer followed by 20 s sonication and 30 s vortexing. Lysates were incubated for 5 min on ice and then spun at 4°C and 10,000*g* for 15 min. Supernatants were collected and used as samples for the next steps. Briefly, on a black 96 well microplate (30296, SPL Life Sciences), a volume of 90 μl of sample was combined with 10 μl of 1 mM L-tryptophan solution followed by 45 min incubation on a microplate shaker set at 100 RPM and 37°C in the dark. A volume of 50 μl of fluorogenic developer solution was added to each sample mixture followed by 3 hr incubation in the dark on a microplate shaker set at 100 RPM and 45°C. NFK 8-point standard curve was used for signal quantification. The plate was read on a Tecan Infinite® 200 PRO in fluorescence mode (402 nm Ex. and 488 nm Em.).

2.7 | Cytokine multiplex assay

The Bio-Plex Pro™ Human Cytokine 27 -plex Assay (M500KCAF0Y, BioRad, Hercules, CA) was used for cytokine quantification in the culture supernatant preserved at −80°C. All reagents were prepared according to the manufacturer's protocol. Briefly, a volume of 50 μl of each sample and standards were added in duplicate to a 96-well plate previously loaded with magnetic beads dissolution. After a 30 min incubation in a microplate shaker set at 850 ± 50 RPM and room temperature (RT), three washing steps were performed using the BioPlex Handheld Magnetic Washer (171020100, BioRad, Hercules, CA). A volume of 25 μl of detection antibodies was added to each well and kept protected from light while shaking at 850 ± 50 RPM for 30 min incubation at RT. After washing, a volume of 50 μl of streptavidin-PE was added to each well and incubated for 10 min with shaking. Beads were resuspended in 125 μl assay buffer and shaken for 30 s at 850 ± 50 RPM. The assay plate was read in a Bio-Plex® 200 System (BioRad, Hercules, CA) using low PMT and RP1 setting. Data were processed using the Bio-Plex Manager™ version 6.2 (Bio-Rad Laboratories, Inc.). Data were expressed as median fluorescence intensities and as concentration (pg/ml) of detected cytokines.

2.8 | Cytoskeleton analysis

BMSCs and ADSCs were fixed in 4% paraformaldehyde solution (15710, Electron Microscopy Sciences) in DPBS 1X and stained with Hoechst 33342 (H3570, ThermoFisher Scientific, Nashville, TN) and ActinRed™ 555 ReadyProbes™ Reagent (R37112, ThermoFisher Scientific), for further analysis of cell cytoskeletal area expansion and elongation, as a plausible indicator of cell adhesion[27] and differentiation[31] induced by the evaluated culture conditions. Fluorescent images were obtained using a ZOE™ Fluorescent Cell Imager (BioRad, Hercules, CA) and analyzed with CellProfiler™. The data obtained were used to generate heat maps of the resulting cytoskeleton analysis.

2.9 | Morphological assessment

BMSCs (3000 cells/cm^2) lot 00182 (RB182, RoosterBio®) and lot 00114 (RB114, RoosterBio®) were seeded and incubated on TCP, 8-L and 9-L substrates for 24 hr. The culture media was replaced with regular growth media supplemented ± IFN-γ and incubated for 24 hr. Cells

were fixed with 4% (wt/vol) paraformaldehyde for 15 min and then rinsed three times with DPBS 1X. Cells were then stained with NucRed (R37106, ThermoFisher Scientific) incubated for 20 min and followed by a 30 min incubation with 20 μM fluorescein isothiocyanate (FITC) Maleimide (62245, ThermoFisher Scientific). Images were captured with ArrayScan VTI HCS Reader (ThermoFisher Scientific) (Figure 5a). Images were then processed using CellProfiler to extract cell features.

2.10 | Multivariate analysis of morphological feature

RStudio was used for multivariate statistical analysis on 14 cell body features that were obtained by processing images through CellProfiler. Cells seeded on each surface were randomized and then the mean of every 2000 cells was taken within a condition. The features from averaged cells were run through partial least squares discriminant analysis (PLS-DA). Predictive models using morphological data were created using PLS-DA.

2.11 | Statistical analysis

Results are presented as mean ± *SEM*. Two-way analysis of variance (ANOVA) was done to detect significant changes for multifactorial analysis. Statistical analysis was performed using the Graph Pad Prism 7.0 software for Windows. A p-value <0.05 was considered statistically significant.

3 | RESULTS

3.1 | Physicochemical characteristics of deposited HEP/COL multilayers

LbL is a method that takes advantage of electrostatic interactions as a function of pH to enable a stacked deposition of oppositely charged polymeric nanolayers. Figure 1a illustrates the procedure used for the generation of HEP/COL stacked multilayers on the surface of a culture vessel of a 96-well plate. Analogous steps were followed employing a dipping technique for layer deposition into silicon wafers used for physicochemical characterization. The resulting surface thickness and coverage depend on the type of polymers used, and both increase with the number of layers deposited. As expected, the examination of the coated surface area on a silicon wafer shows a positive correlation between the number of layers deposited and the percentage of surface area covered (Figure 1b). Stacks composed of eight layers or more covered over 90% of the surface area. Based on this information stacks of eight layers of HEP/COL were selected for physicochemical characterization. SPR analysis on the peak min angle of the gold-coated sensor during HEP/COL assembling support the formation of the polymeric multilayers. The sensogram (Figure 1c) confirms the formation of eight layers of alternating building blocks of HEP and COL, where it can be observed that the growth kinetics of the HEP/COL multilayers is highly dependent by the deposition of COL. Chemical composition of layers deposited on silicon substrates were characterized using the IR-VASE® instrument, as previously

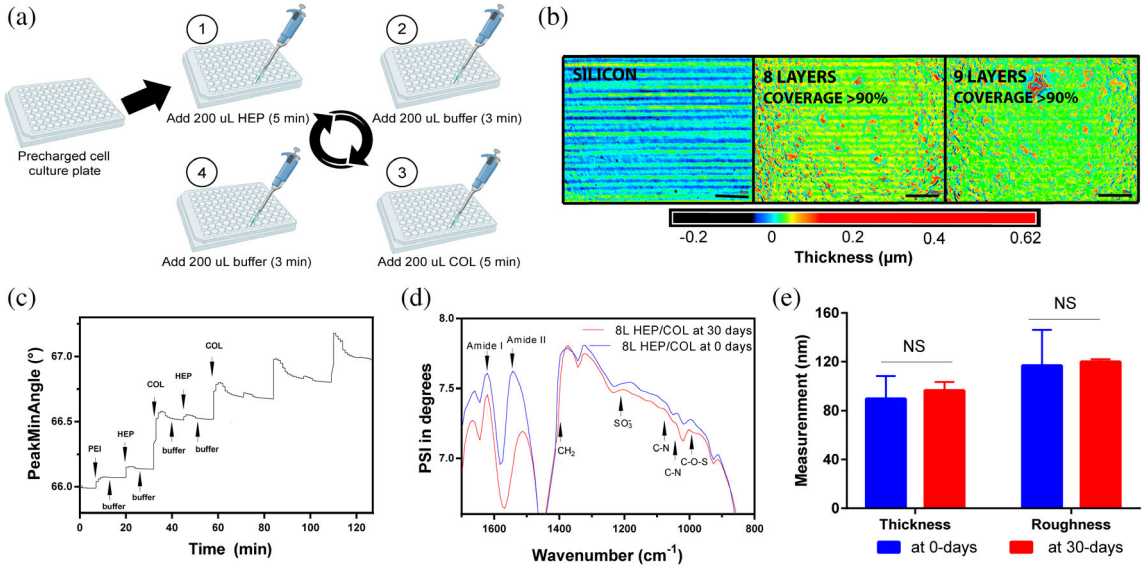

FIGURE 1 Representation of HEP/COL deposition of the desired number of layers on cell culture plates and layers characterization. (a) To produce HEP/COL multilayers on cell culture plates, each culture well was positively charged by depositing 200 μl of PEI for 15 min, followed by 3 min of buffer washing. Then, the deposition of HEP and COL began by adding a negatively charged heparin solution, followed by the positively charged collagen solution in a cyclic procedure, with 3 min washing steps in between. This figure was created with BioRender.com. (b) Surface coverage of sequentially deposited HEP/COL multilayers, images (0.063 mm^2) using a silicon wafer as a baseline reference. Changes in color indicate an increase in surface thickness. The red color corresponds to high peaks detected on the surface. Scale bar = 50 μm. (c) SPR sensogram of HEP/COL multilayer formation. (d) IR-VASE spectrum of eight deposited multilayers at 0 and 30 days from fabrication after storage at 22°C and 40% relative humidity. (e) The thickness and roughness of eight layers (HEP/COL) measured after 0 and 30 days of fabrication. Data represent the mean ± *SD*, n = 3. COL, collagen I; HEP, heparin; PEI, polyethyleneimine; SPR, surface plasmon resonance

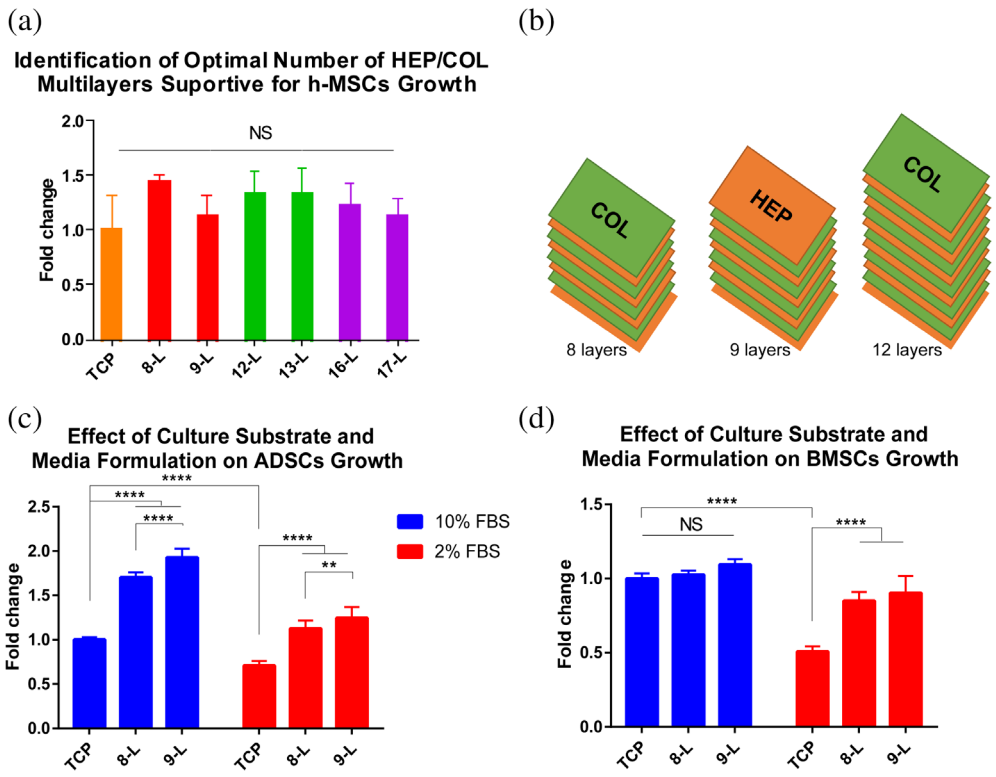

FIGURE 2 Cell viability on culture substrates at 5 days. (a) Cell viability of ADSCs on TCP and different constructions of HEP/COL multilayers cultured with media containing 2% FBS. Data represent the mean relative values to TCP ± STDEV of $n = 4$ samples. One-way ANOVA was used for statistical analysis among the multiple conditions. (b) Representation of the number of layers and ending material, odd layers end in HEP while even layers end in COL. (c) Viability of ADSCs supplemented with 10 and 2% FBS cultured on TCP (control), eight and nine layers as selected from preliminary experiments with Lonza ADSCs, and (d) Viability of BMSCs supplemented with 10 and 2% FBS cultured on TCP, eight and nine layers. Data are normalized to TCP at the highest media formulation on each plot and represent the mean ± *SEM* of $n = 10$ from two independent experiments. Two-way ANOVA was used for data analysis. Statistical significance is represented by asterisks (*) as follows: $^{**}p < 0.01$ and $^{****}p < 0.0001$. ADSCs, adipose-derived stromal cells; BMSCs, bone marrow-derived mesenchymal stromal cells; COL, collagen I; HEP, heparin; TCP, tissue culture plastic

described.[29,30] Measurements performed at 0 and 30 days post-fabrication are shown in Figure 1d. Distinctive functional groups, such as amide I (1700–1,600 cm^{-1}) and amide II (1600–1,500 cm^{-1}) were identified on the constructed layers confirming the presence of the structural collagen I triple helix and heparin.[30] Functional peaks, including the CH_2 scissoring near 1400 cm^{-1}, the C—N stretching at 1070 and 1040 cm^{-1}, and the C—O—S stretching vibrations at approximately 950 cm^{-1} were identified as described in the literature,[30] thus confirming that HEP/COL layers were successfully deposited and preserved their functional groups. The thickness of the stacked layers was similar between samples (Figure 1e), with an average thickness of 90 nm, which is in concordance to what was previously reported by Castilla et al[29] for layers examined immediately after fabrication at 25°C. Layers analyzed at 30 days postfabrication retained their functional groups and showed a minimal increase in thickness (~96 nm), which can be attributable to moisture absorption from the environment. This agrees with a previous study supporting the time-preservation of the chemical properties of polymeric multilayers generated by the LbL method.[32] Substrate roughness had an average of 118 nm for both time points indicating that this property was not affected during storage.

To confirm that HEP/COL multilayers have a higher protein absorption capacity than TCP, the absorption of bovine serum albumin (BSA) conjugated to Texas Red™ was estimated as a function of the total amount of deposited layers. The surface bound portion of BSA was indirectly quantified from fluorescent measurements of initial total and unbound protein concentrations in aqueous solution. As expected, the absorption of BSA was higher for both COL-ending and HEP-ending substrates as compared to TCP (Figure S1). Substrates that the surface top layer ended in HEP (7-L, 9-L, 11-L, and 13-L) showed the highest protein absorption with an average of 50 and 33% more BSA than TCP and COL-ending substrates (8-L and 12-L) respectively. The enhanced absorption on HEP was expected since it is a polysaccharide with many functional groups and motifs that act as binding sites for peptides and proteins.[33-35]

3.2 | Multivariate analysis of HEP/COL multilayers effect on h-MSCs growth

Growth factor supplementation is a major cost driver and supply barrier for the scale up process of cell culture.[36] Thus, culture substrates

employed for cell culture applications should minimized the added cost to the culture process. Our previous studies show that substrates made of 12 and 13 layers of HEP/COL perform better than TCP in supporting viability, adhesion, and cytokines secretion for h-MSCs cultured in media with 20% FBS, and IFN-γ stimulation.[29] However, the examination of cell growth as a function of the number of layers was not determined. To identify the minimum number of deposited layers for enhanced growth, ADSCs were cultured on HEP/COL multilayers deposited as stacks ranging from 8 to 17 layers in reduced serum media for 5 days. Results from this exploratory study indicate that cell growth was enhanced in HEP/COL multilayers indistinctly of the number of layers employed (Figure 2a). Thus, substrates with a minimum of eight and nine layers (Figure 2b) were selected for the subsequent set of cell culture studies. Figures 2c,d summarizes the results of cell growth for ADSCs and BMSCs one donor each, after been cultured on HEP/COL substrates using culture media supplemented with either 2 or 10% serum for 5 days. Figure 2c shows that HEP/COL multilayers improve the growth of ADSCs independently of the media

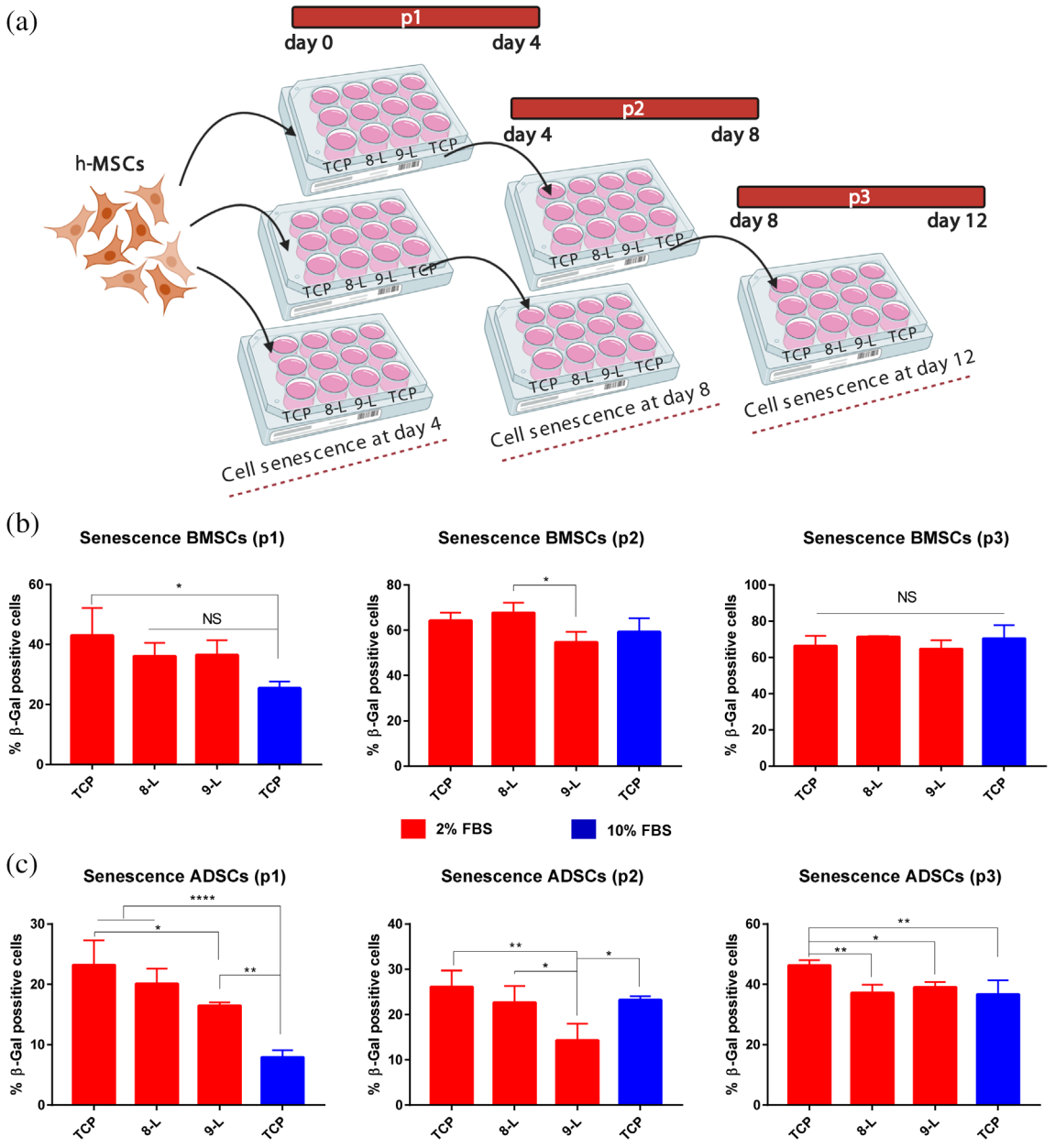

FIGURE 3 Examination of cell senescence on HEP/COL multilayers. (a) h-MSCs were seeded on three well plates. Every 4 days, a cell plate was assessed for senescence while the remaining plates where harvested and replated in similar culture conditions. This figure was created with BioRender.com. (b,c) The percentage of β-galactosidase positive BMSCs (b) and ADSCs (c) cultured on TCP, 8-L and 9-L substrates was examined over three sequential passages. Data represents the mean ± STDEV of $n = 4$ samples. Data analysis was performed using one-way ANOVA with multiple comparisons among culture conditions. *$p < 0.05$, **$p < 0.01$, and ****$p < 0.0001$. ADSCs, adipose-derived stromal cells; BMSCs, bone marrow-derived mesenchymal stromal cells; COL, collagen I; h-MSCs, human mesenchymal stromal cells; HEP, heparin; TCP, tissue culture plastic

formulation as compared to TCP. Cell growth in media supplemented with 2% FBS was equivalent to standard TCP cultures using 10% serum. For BMSCs (Figure 2d), HEP/COL multilayers had a small increase in cell growth at 10% FBS, but a significant increase at 2% FBS concentration reaching values equivalent to those obtained in 10% FBS.

Additional cell growth studies were performed to determine potential synergistic effects based on the contributions of each single component substrate. Single component coatings were generated by the spin-coating method and characterized as described for HEP/COL layers. Single component coatings had thicknesses of 90 and 140 nm for collagen I and heparin respectively (Figure S2) which are close to that obtained for HEP/COL multilayers tested herein. Examination of cell viability at 5 days shows that single COL coatings enhanced cell growth by up to 34% as compared to TCP conditions for both cell lines, where only statistical significance was found for ADSCs but not for BMSCs (Figure S2). On the other hand, single component HEP films were not supportive of cell growth and had a decrease of 50% or higher in cell expansion as compared to TCP. The enhanced cell growth observed on single component COL coatings fell short by up to 50% as compared to multilayers ending in HEP (Figure 2c). Thus, the data supports a synergistic effect of combined HEP and COL alternating stacked layers on cell growth.

3.3 | Impact of HEP/COL multilayers on h-MSCs senescence

In vitro expanded cells experience metabolic and genomic changes that ultimately impair the regenerative capacity of cells marked by an increase in the population of senescent cells.[37] In this work, cell senescence was examined to determine whether HEP/COL multilayers in combination with a reduced serum content (Figure 3) had a negative impact on cell propagation after sequential passages. Cell senescence was examined in h-MSCs cultured on TCP, 8-L and 9-L and compared with cells cultured in TCP in media supplemented with 2% FBS. Cells cultured on TCP supplemented with media containing 10% FBS was used as a positive reference control for high cell propagation rate and thereby low senescence. For BMSCs, an average of 65% of cells were β-galactosidase positive after three passages indistinctly of the culture surface or serum content. For

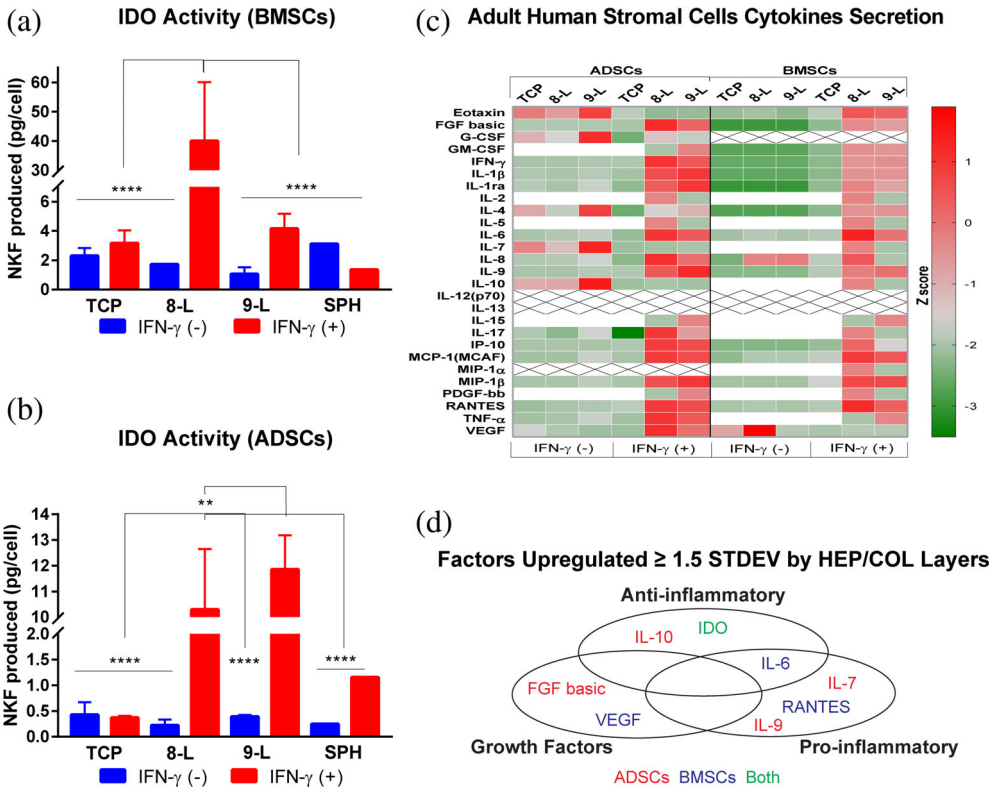

FIGURE 4 Cells immunomodulatory potential, (a) Intracellular IDO activity for BMSCs as a measure of picograms of N-Formylkynurenine (NFK) produced by cells. (b) NFK related IDO activity for ADSCs. Data represent the mean ± *SEM* of $n = 4$ from two independent experiments. Data were analyzed using two-way ANOVA. $^{**}p < 0.01$ and $^{****}p < 0.0001$. (c) Heatmap showing the Z-score values of 27 human cytokines in response to culture surfaces and conditioned media. Data represent the mean of $n = 4$ from two independent experiments. Cytokines in white means that Z-scores were under the lower limit set as −3.5 STDEV, while for grey cross marked cytokines, Z-scores could not be determined. (d) Summary of factors that were upregulated by 1.5 or higher STDEV by HEP/COL multilayers on h-MSCs. ADSCs, adipose-derived stromal cells; BMSCs, bone marrow-derived mesenchymal stromal cells; COL, collagen I; h-MSCs, human mesenchymal stromal cells; HEP, heparin; IDO, indoleamine 2, 3-dioxygenase

ADSCs, a small but significance reduction was observed in the number β-galactosidase positive on HEP-ending layers (9-L) as compared to TCP at 2% FBS. Overall, our results indicate that cell senescence was progressively increasing for all culture conditions and this trend increased with each passage. Thus, it can be concluded that HEP/COL substrates do not had a negative impact in the cell senescence of the h-MSCs examined.

3.4 | Immunomodulatory potential of h-MSCs on HEP/COL multilayers

3.4.1 | Intracellular IDO activity

IDO secretion is known to be one of the mechanisms orchestrated by h-MSCs to suppress the activity of T-cells.[38] IFN-γ is an inflammatory factor secreted by natural killer (NK) cells and T lymphocytes[39] used to examine the secretory potency of h-MSCs in response to inflammatory stimulus. Intracellular IDO activity was examined in h-MSCs cultured on TCP and HEP/COL multilayers at 5 days post-stimulation with IFN-γ in media with 2% serum. Cell aggregates (spheroids) were included in this analysis as a positive control for enhanced IDO production as compared to 2D culture conditions in TCP.[40] IDO levels were determined by the amount of NFK produced (pg/cell), which is known to be an intermediate product in the enzymatic activity of IDO on tryptophan (Trp).[41] Results for IDO activity are summarized in Figures 4a,b. Multilayers ending in COL consistently showed enhanced intracellular levels (>20-fold increase) of IDO upon stimulation with IFN-γ as compared to TCP and spheroids. Multilayers ending in HEP also promoted amelioration of intracellular IDO post-stimulation with IFN-γ. However, the levels of IDO were found to be statistically significant in ADSCs only, whereas for BMSCs, IDO levels were 10-fold lower as compared to 8-L.

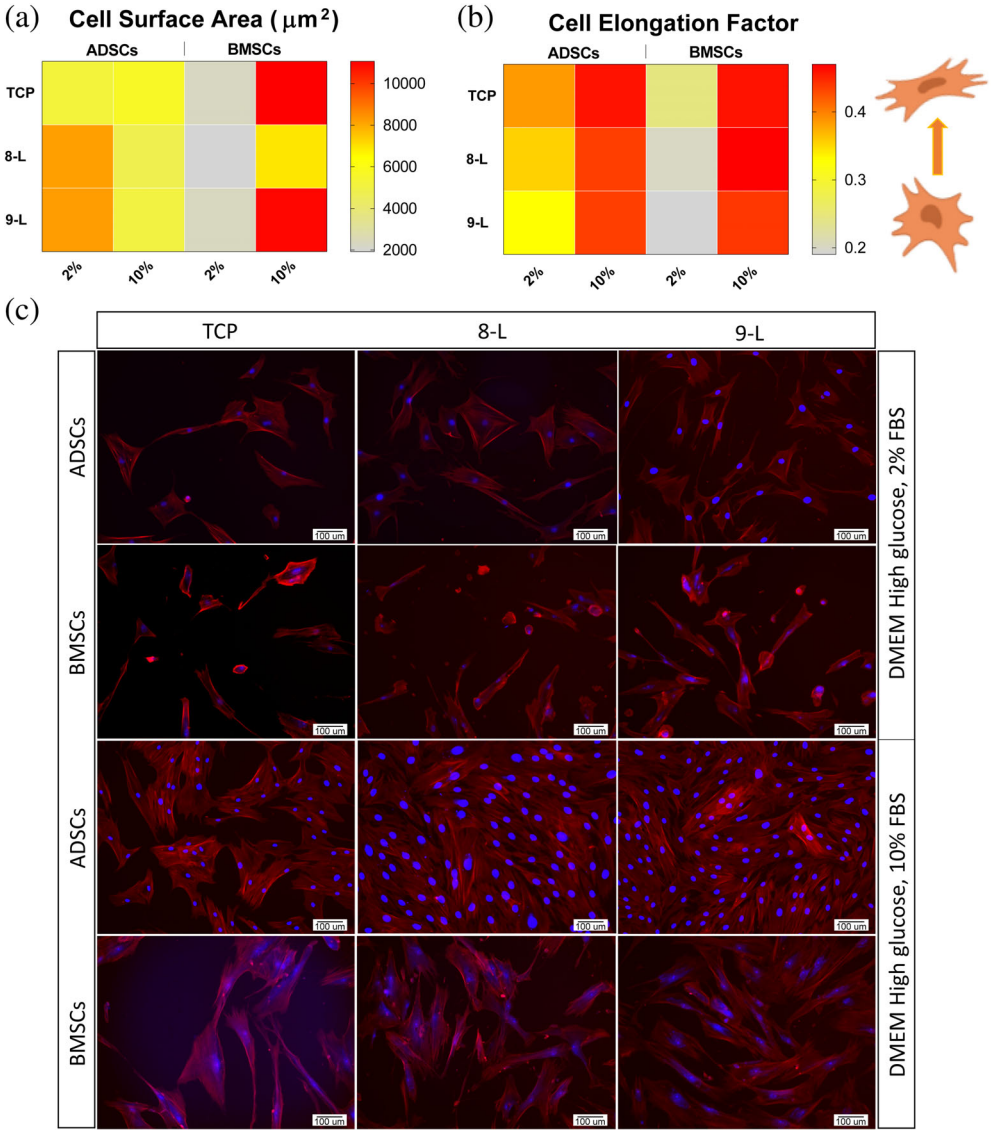

FIGURE 5 h-MSCs morphological aspects, (a) Changes in h-MSCs cytoskeleton surface area induced by culture conditions, (b) impact of the culture conditions in h-MSCs elongation, and (c) stained merged images (nuclei (blue) and cytoskeleton (red)) of h-MSCs cultured on the studied set of culture substrates after five days culturing in basal media supplemented either with 2 or 10% FBS. h-MSCs, human mesenchymal stromal cells

3.4.2 | Cytokine profile

To quantify changes at the secretome level, soluble concentrations of 27 analytes were measured in the cell supernatant from ADSCs and BMSCs previously cultured as monolayers on TCP, and HEP/COL deposited multilayers, with and without IFN-γ stimulation at 5 days. Most cytokines examined were detected and abundant in HEP/COL multilayered substrates but secreted at low levels or not detected in IFN-γ unstimulated TCP cultures. The Z-score value was calculated per for each analyte per cell donor and summarized in a heatmap format as shown on Figure 4c. Concentration values relative to total cell counts are shown in Tables S1 and S2 of supplemental Information. For both, ADSCs and BMSCs, the concentration of secreted cytokines was higher on HEP/COL multilayers under IFN-γ stimulation. However, it was also noticed that for some cytokines the HEP/COL multilayers were enough to enhance factor concentration without the need for IFN-γ immune stimulation. Such as in the case of Eotaxin, G-SCF, IL-4, IL-7, and IL-10, which interestingly were noticed to be more secreted by ADSCs when cultured in 9-L in the absence of exogenous IFN-γ.

HEP/COL multilayers enhanced the secretion of growth factors important for wound healing (VEGF),[42] skeletal tissue repair (PDGF-bb),[43] and proliferation (FGF-basic).[44] In addition to growth factors, several cytokines were overexpressed that are of therapeutic value. For example, IL-6 which is involved in both pro- and anti-inflammatory activities[45,46]; IL-1ra, an anti-inflammatory cytokine that antagonizes the activity of IL-1 by blocking its receptor, thus reducing articular inflammation and cartilage damage[47]; IL-4, a cytokine which plays a key role in humoral and adaptive immunity[48]; TNF-α, a cytokine related to immune system response against tumor progression[49]; and IL-10, a prominent anti-inflammatory cytokine mostly secreted by B cells to maintain the normal immune homeostasis.[50] As summarized in Figure 4d, the enhanced secretome effect was more notable in ADSCs than BMSCs. As potency is linked to higher levels of cytokines secretion,[51] this data suggests that ADSCs are more potent than BMSCs.

3.5 | Multivariate analysis of HEP/COL multilayers effect on h-MSCs morphology

3.5.1 | Examination of cell elongation and surface area

Cell morphological features, including cytoplasmic elongation and cell surface expansion, are cell adhesion indicators[27] used for quality control of h-MSCs differentiation.[31] Also, other studies have reported that the cell morphological features like cell perimeter, cell Feret diameter, and nucleus/cytoplasm-ratio correlate well with the immunosuppressive capacity of IFN-γ stimulated h-MSCs.[52] An image-based analysis of cytoskeleton expansion and elongation (aspect ratio) was performed as a function of the culture substrates (Figures 5a,b). High magnification images of cytoplasmic stained cells are presented in Figure 5c. Upper and lower intervals for cell surface area were dependent on the media formulations. BMSCs showed to be markedly affected by media formulation by showing the smallest cytoskeleton expansion indistinctly of the culture substrate in 2% serum and the

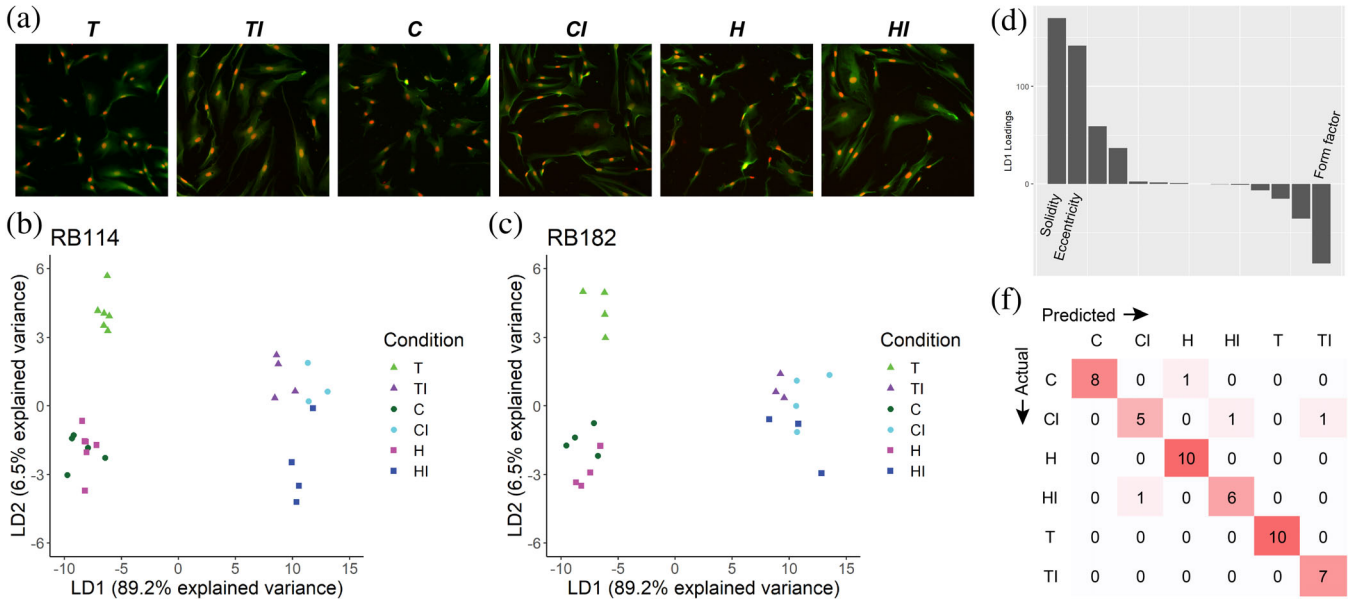

FIGURE 6 MSC morphological assessment. (a) Representative images of h-MSCs seeded on different surfaces without stimulation of IFN-γ. The cell body was stained with FITC Maleimide (green), and nuclei with NucRed (red). (TCP (T), 8-L (C), 9-L (H)) and with stimulation of IFN-γ (TCP (TI), 8-L (CI), 9-L (HI)). (b,c) PLS-DA on morphological features of cells seeded on different surfaces with and without stimulation of IFN-γ shows separation. (d) LD1 loadings solidity, eccentricity, and form factor features have the largest contribution. (e) Confusion matrix showing the accuracy of prediction for the PLS-DA model. IFN-γ, interferon-γ; h-MSCs, human mesenchymal stromal cells; PLS-DA, partial least squares discriminant analysis; TCP, tissue culture plastic

highest cytoskeletal surface expansion when cultured on TCP and 9-L at 10% serum (Figure 5a).

A rounded cell shape is defined by a cell elongation factor closer to zero, while the closer the value to one indicates an elongated cell morphology (Figure 5b). Despite not being easily identifiable differences in elongation from cell micrographs (Figure 5c), ADSCs and BMSCs were more elongated when cultured in media supplemented with 10% FBS, indicating that the effects imparted on cell morphological changes are strongly influenced by the media formulations instead of the culture substrates.

3.5.2 | Morphological assessment and PLS-DA analysis in response to IFN-γ stimulation

To identify the morphological differences induced in cells by different growth surfaces and during immune activation, we tested two BMSCs donors seeded on different surfaces during normal culture expansion and under IFN-γ immune stimulation. Representative images of h-MSCs seeded on different surfaces with and without IFN-γ stimulation are presented in Figure 6a. Figures 6b,c illustrate the first two components obtained from a PLS-DA, with each cell colored according to its growth surface type with and without IFN-γ stimulation. The largest effect was observed between all cells after IFN-γ stimulation. Interestingly, IFN-γ stimulation altered cell morphology in the same fashion for all surfaces, suggesting that IFN-γ immune stimulation had a stronger impact on the cell morphology than the tested growth substrates. The majority of this morphological effect induced by IFN-γ stimulation is accounted for by LD1 (89% variance). As observed in the loadings plot, the largest changes in morphological features that can be attributed predominantly to the IFN-γ stimulation (71% of the total loading) (Table S3) are an increase in solidity and eccentricity and a decrease in form factor (Figure 6d). These lead to elongation and spreading of cells, which could have a positive correlation with immunosuppressive activity, as has been suggested by others.[53] Cells from donor RB114 stimulated with INF-γ on the 9-L are distinctly separated from cells seeded in a normal tissue culture plate and from the 8-L surface along LD2. This separation is not so distinct in the RB182 cell donor, suggesting that there is heterogeneity between h-MSCs donors in their responses to the surfaces.

Although LD2 (6.5% variance) accounted for less of the observed separation between samples than LD1, under expansion culture conditions, h-MSC morphology was distinct between tissue culture plastic and the LbL coated surfaces for both donors (Table S4, Figure S3). This result indicates a change in morphological features on the HEP/COL multilayers, suggesting that engagement with bioactive ligands on the 8-L and 9-L surfaces likely alters underlying biological function in the cells. LD2 morphological loadings find features indicative of cell length and spread such as eccentricity, solidity, and mean radius contribute 72% to the distribution along LD2, suggesting that h-MSCs trend toward being less elongated and with a smaller radius on the COL and HEP surfaces. Variability was also observed within the data from each group, but many groups do not form tight clusters indicating diversity in their morphological response to growth substrate and immune stimulation. Overall, our PLS-DA classifier performed with ~92% accuracy to classify cell growth substrate and immune response (Figure 6e) using a leave-one-out cross-validation approach.

4 | DISCUSSION

Multilayered HEP/COL substrates have demonstrated to have a positive impact on h-MSCs growth and secretome. The enhanced effect on cell growth was captured for both cell donors and can be attributed to the biochemistries of COL and HEP components when presented simultaneously in a substrate. Although the mechanisms associated with the observed changes in cell behavior were not the focus of this study, probably both integrin signaling, and growth factor /cytokine sequestration by HEP/COL macromolecules played a role. Our assessment on BSA absorption (Figure S1) confirmed that both 8-L and 9-L had a higher protein absorption capability than TCP. This agrees with previous findings reporting HEP as a growth factor binding sulfated glycosaminoglycan.[33-35] In our system, the growth of h-MSC was supported on HEP/COL multilayers at 2% serum concentration at levels equivalent to those observed in standard culture conditions (TCP and 10% FBS). Thus, it is very likely that HEP layers enriched the local availability of cell-secreted and exogenous supplemented factors to contribute to the observed growth enhancement under reduced serum conditions.

In addition to HEP, COL also contributed to the observed changes in cell behavior as our results showed that HEP as single component had a more of an inhibitory effect on cell growth (Figure S2). Our studies using COL coatings reinforced its role in stimulating cell growth particularly in reduced serum condition. Extracellular receptors such as integrins are a potential mechanism regulating the observed cell behavior on COL containing substrates. Cell cycle progression is linked to a synergistic role between tyrosine kinase growth factor receptors (RTKs) and integrins,[54] where these last play a major role by promoting the activation of RTKs with their ligands. Given the observation that substrates containing HEP and COL alternating stacked layers outperformed single component substrates in supporting cell growth, the mechanisms supportive of such interaction should be elucidated to identify alternative strategies to stimulate cell growth in a low growth factor environment such as culture systems that employ reduced growth factor media formulations in combination with synthetic substrates or suspended cell cultures.

Various are the strategies proposed to overcome expansion related cell senescence. From hypoxic culture preconditioning,[55] found to be highly effective in inhibiting cell senescence, to gene editing approaches for improved telomerase expression.[56] However, cells expanded under low oxygen concentration present chromosomal instability,[57] while enhanced telomerase activity induces an accelerated osteogenic differentiation of h-MSCs[58] restricting its use to tissue engineering applications. Our studies show that HEP/COL

multilayers did not impaired the replicative capacity of h-MSCs over a period of 12 days. As the focus of this study is the stimulation of cell growth and immunosuppressive secretome of h-MSCs, both tightly associated to the undifferentiated and highly proliferative status of the cells, then we conclude that these HEP/COL multilayers substrates are appropriate for cell culture applications in which cell-derived factors are of interest within a short-time window. Yet, these substrates did not show a significant reduction in the proportion of senescent cells, as the percentage of β-galactosidase positive h-MSCs was similar among all culture conditions at the end of the study. Thus, cell culture related senescent is still a challenge in the field particularly for long-term cell expansion process.

There is a need for culture strategies that can substantially reduce the time and cost of cell manufacture of h-MSCs. Within the cost of goods for cell manufacturing, raw materials represent up to 36% of the total, with cell growth media components accounting for near to 50% of such costs.[7] Our assessment of the cost of raw materials indicates that HEP/COL culture substrates are a potential strategy for reducing the cost of cell expansion in h-MSCs. The cost of culture media and raw materials employed for the fabrication of COL/HEP substrates was determined based on academic pricing. Results indicate savings of an average of 42% (Table S5 of supplemental information) when comparing 10% serum on TCP versus 2% serum + COL/HEP substrates. Such costs can be further reduced with the use of automated instrumentation and reuse of solutions during the dipping process.

As mentioned before, one of the therapeutic properties of clinical interest of undifferentiated h-MSCs is their immunosuppressive potential. The immunosuppressive capability of h-MSCs is of increasing interest due to their growing demand in clinical applications for inflammatory conditions such as multiple sclerosis and type 1 diabetes, among others.[5,6] in vivo h-MSC secretion of soluble factors like prostaglandin E2 (PGE2), tumor growth factor β (TGF- β), and IDO regulate innate and adaptative immune responses to suppress inflammation[39] by mediating macrophages polarization, mast cell degranulation, neutrophils apoptosis, NK cells activation, and CD4+ activation and polarization toward th1 and th17 cells. Such therapeutic properties rely mostly on the secretion of soluble factors by undifferentiated h-MSCs.[59] Several strategies have been used to enhance their immunomodulatory potential. Cell incubation with either immunosuppressive drugs[17] or immunostimulatory cytokines, among which IFN-γ,[59,60] have been reported to increase h-MSCs regulatory activity by reducing the proliferative index of co-cultured immune cells. Here, we showed that the HEP/COL multilayered substrates generated stimulate enhanced IDO levels and cytokine secretion associated to immunomodulation potency of h-MSCs. The enhanced intracellular levels of IDO observed particularly on COL-ending substrates (8-L) could be supported by integrin-mediated IDO signaling. The canonical mechanism for IDO production is supported by the combined activation of the INF-γ induced JAK/STAT[61] pathway, and the growth factors induced mitogen-activated protein kinase (MAPK) pathway. MAPK pathway has been shown to be activated by integrin signaling in mammalian cells cultured on collagen substrates,[62] thus representing a potential unexplored mechanism for IDO stimulation. The difference in IDO levels between both cell lines cultured on 9-L (higher for ADSCs than for BMSCs) could be related to differences in the tissue of origin. From the literature, it is known that adipose tissue is rich in mast cells which are associated with heparin production.[63] While the presence of mast cells in the bone marrow is low or rare, and their abundance is associated with bone marrow diseases like mastocytosis, chronic lymphocytic leukemia, and non-Hodgkin lymphoma among others.[64] Moreover, the enhanced secretion of five cytokines by ADSCs in the absence of exogenous IFN-γ, promoted by 9-L surfaces reinforce the potential connection to the high heparin content on the tissue of origin of ADSCs and the reminiscence of interactions with these ECM-like substrates. On the other hand, and consistently to what was pointed out previously, multilayers ending in HEP had little effect on BMSCs on the absence of IFN-γ stimulation.

One of the main concerns for h-MSC based therapies is the definition and assessment of critical quality attributes for cell bioactivity, soluble factors like the studied herein have been supported by a wide group of reported IND submissions.[3] In-line and noninvasive assessments of cell behavior during the cell manufacturing process are required for fast tuning of the culture parameters and monitoring of the cell health status. This will allow for batch quality assessment while minimizing time and raw materials consumption.[65] Among the potential non-invasive cell assays, optical tools are a good candidate due to their compatibility with high throughput acquisition of data from small cell-samples, while reducing expenses related to fluorogenic immunoassays. In our studies, distinct cell morphological aspects were captured for cell grown on HEP/COL multilayers +/− IFN-γ. This morphological change correlated with an enhanced immunomodulatory state in cells grown on 9-L[52,53] based on enhanced cell secretome. Our computer-aided evaluation on cells morphological features was capable to detect changes at both levels; the conditioned by media formulation either with or without IFN-γ. Although, the impact on the multipotentiality and long-term effects in h-MSCs is out of the scope of this study, the data indicates that culture-related morphological features could be associated to differences in h-MSC functional potential.

Despite the positive impact of HEP/COL multilayers substrates in h-MSCs cultures, there are some concerns that may limit its wide application in cell manufacture. HEP and COL type I are both commercial and clinical products,[66,67] but their xenogeneic derivation becomes a concern according to the U.S. Food and Drug Administration (FDA) guidance for human somatic cell-based IND applications.[68] A potential strategy to address this limitation, is to identify peptide sequences in COL and HEP relevant to cell adhesion and protein binding that can be incorporated into synthetic culture systems. A synthetic substrate containing a cocktail of cross-linked COL peptides and HEP fragments may be sufficient to stimulate the growth and secretory capacity of h-MSCs while reducing the risk of contaminants from animal-derived products. Yet the cost of such synthetic system needs to be carefully balanced to avoid increasing the overall cost while maintaining or outperforming the observed benefit of the combined natural components.

Overall, these results demonstrate that HEP/COL multilayers can be used to harness the intrinsic potential of h-MSCs to secrete growth factors and other proteins of therapeutic value. This is important as HEP/COL multilayers allowing cells the ability to potentiate their immunosuppressive properties, becoming a promising strategy to improve outcomes achieved by merely pre-stimulation with pro-inflammatory cytokines.[60] The validation of HEP/COL multilayers as an enhancer in functional immunosuppressive assays will be of relevance for their incorporation in potency assays.

5 | CONCLUSIONS

The current work provides evidence that HEP/COL multilayers support cell growth stimulation at reduced serum conditions while enhancing IDO production and cytokines secretion upon IFN-γ stimulation. These substrates reduce the need for frequent growth factor supplementation in cultures without negatively affecting cell senescence rates supporting their value for cell culture applications. Changes in cell morphological features were captured by a computational model that could relate to differences in h-MSC functional potential. The understanding of h-MSCs morphological signature in the context of biological function will complement the functional characterization of h-MSCs for clinical application. The ability to employ label-free methods to measure cell potency will enable high-throughput screening of potent h-MSCs on LbL produced HEP/COL substrates.

ACKNOWLEDGMENTS

We want to thank Dr. Andres Garcia who provided access to laboratory facilities and instrumentation at the Georgia Institute of Technology. We also thank Integra Life Sciences for generously donating the collagen I sponge used for the generation of layers and cellular studies. This work was accomplished through the funding support from NSF Engineering Research Center for Cell Manufacturing Technologies No. EEC-1648035 and partial support from NIH PR-INBRE No. P20 GM103475-15 and NSF- EPSCoR II CAWT No. OIA-1849243.

CONFLICT OF INTEREST

The authors declare no potential conflict of interest.

ORCID

Maribella Domenech https://orcid.org/0000-0001-7061-8090

REFERENCES

1. Zou J-P, Huang S, Peng Y, et al. Mesenchymal stem cells/multipotent mesenchymal stromal cells (MSCs). *Int J Low Extrem Wounds*. 2012;*11*:244-253.
2. Castilla-Casadiego DA, Reyes-Ramos AM, Domenech M, Almodovar J. Effects of physical, chemical, and biological stimulus on h-MSC expansion and their functional characteristics. *Ann Biomed Eng*. 2019;*47*:1-17.
3. Mendicino M, Bailey AM, Wonnacott K, Puri RK, Bauer SR. MSC-based product characterization for clinical trials: an FDA perspective. *Cell Stem Cell*. 2014;*14*:141-145.
4. Meirelles L d S, da Silva Meirelles L. Mesenchymal stem cells reside in virtually all post-natal organs and tissues. *J Cell Sci*. 2006;*119*:2204-2213.
5. Dulamea A. Mesenchymal stem cells in multiple sclerosis - translation to clinical trials. *Med Life*. 2015;*8*:24-27.
6. Bosi CA, Lanzoni G, Pugliese A. Clinical trials of mesenchymal stem cell transplantation in patients with type 1 diabetes and systemic lupus erythematosus: is it time for larger studies? *CellR4*. 2016;*4*(5):e2134.
7. Lipsitz YY, Milligan W, Fitzpatrick I, et al. A roadmap for cost-of-goods planning to guide economic production of cell therapy products. *Cytotherapy*. 2017;*19*:1383-1391.
8. Simaria AS, Hassan S, Varadaraju H, et al. Allogeneic cell therapy bioprocess economics and optimization: single-use cell expansion technologies. *Biotechnol Bioeng*. 2014;*111*:69-83.
9. Kim HJ, Park J-S. Usage of human mesenchymal stem cells in cell-based therapy: advantages and disadvantages. *Dev Reprod*. 2017;*21*:1-10.
10. Jenkins MJ, Farid SS. Human pluripotent stem cell-derived products: advances towards robust, scalable and cost-effective manufacturing strategies. *Biotechnol J*. 2015;*10*:83-95.
11. Want AJ, Nienow AW, Hewitt CJ, Coopman K. Large-scale expansion and exploitation of pluripotent stem cells for regenerative medicine purposes: beyond the T flask. *Regen Med*. 2012;*7*:71-84.
12. Hanley PJ, Mei Z, Cabrera-Hansen MG, et al. Manufacturing mesenchymal stromal cells for phase I clinical trials. *Cytotherapy*. 2013;*15*:416-422.
13. Gottipamula S, Muttigi MS, Kolkundkar U, Seetharam RN. Serum-free media for the production of human mesenchymal stromal cells: a review. *Cell Prolif*. 2013;*46*:608-627.
14. Ng F, Boucher S, Koh S, et al. PDGF, TGF-beta, and FGF signaling is important for differentiation and growth of mesenchymal stem cells (MSCs): transcriptional profiling can identify markers and signaling pathways important in differentiation of MSCs into adipogenic, chondrogenic, and osteogenic lineages. *Blood*. 2008;*112*:295-307.
15. Agata H, Watanabe N, Ishii Y, et al. Feasibility and efficacy of bone tissue engineering using human bone marrow stromal cells cultivated in serum-free conditions. *Biochem Biophys Res Commun*. 2009;*382*:353-358.
16. Rodrigues CAV, Fernandes TG, Diogo MM, da Silva CL, Cabral JMS. Stem cell cultivation in bioreactors. *Biotechnol Adv*. 2011;*29*:815-829.
17. Girdlestone J, Pido-Lopez J, Srivastava S, et al. Enhancement of the immunoregulatory potency of mesenchymal stromal cells by treatment with immunosuppressive drugs. *Cytotherapy*. 2015;*17*:1188-1199.
18. Samsonraj RM, Rai B, Sathiyanathan P, et al. Establishing criteria for human mesenchymal stem cell potency. *Stem Cells*. 2015;*33*(6):1878-1891.
19. Kuraitis D, Giordano C, Ruel M, Musarò A, Suuronen EJ. Exploiting extracellular matrix-stem cell interactions: a review of natural materials for therapeutic muscle regeneration. *Biomaterials*. 2012;*33*:428-443.
20. Yeo GC, Weiss AS. Soluble matrix protein is a potent modulator of mesenchymal stem cell performance. *Proc Natl Acad Sci U S A*. 2019;*116*(6):2042-2051.
21. Saei-Arezoumand K, Alizadeh E, Pilehvar-Soltanahmadi Y, Esmaeillou M, Zarghami N. An overview on different strategies for the stemness maintenance of MSCs. *Artif Cells Nanomed Biotechnol*. 2017;*45*:1255-1271.
22. Lee JH, Luo X, Ren C, et al. A Heparan sulfate device for the regeneration of osteochondral defects. *Tissue Eng Part A*. 2019;*25*:352-363.

23. Monge C, Almodóvar J, Boudou T, Picart C. Spatio-temporal control of LbL films for biomedical applications: from 2D to 3D. *Adv Healthc Mater*. 2015;*4*:811-830.
24. Boudou T, Crouzier T, Ren K, Blin G, Picart C. Multiple functionalities of polyelectrolyte multilayer films: new biomedical applications. *Adv Mater*. 2010;*22*(4):441-467.
25. Picart C, Mutterer J, Arntz Y, Voegel JC, Schaaf P, Senger B. Application of fluorescence recovery after photobleaching to diffusion of a polyelectrolyte in a multilayer film. *Microsc Res Tech*. 2005;*66*(1):43-57.
26. Mhanna RF, Vörös J, Zenobi-Wong M. Layer-by-layer films made from extracellular matrix macromolecules on silicone substrates. *Biomacromolecules*. 2011;*12*(3):609-616.
27. Muzzio NE, Pasquale MA, Gregurec D, et al. Polyelectrolytes multilayers to modulate cell adhesion: a study of the influence of film composition and polyelectrolyte Interdigitation on the adhesion of the A549 cell line. *Macromol Biosci*. 2016;*16*:482-495.
28. Fichtner M, Claus C, Lessig-Owlanj J, Arnhold J, Reibetanz U. The application of LbL-microcarriers for the treatment of chronic inflammation: monitoring the impact of LbL-microcarriers on cell viability. *Macromol Biosci*. 2015;*15*:546-557.
29. Castilla-Casadiego DA, García JR, García AJ, Almodovar J. Heparin/collagen coatings improve human mesenchymal stromal cell response to interferon gamma. *ACS Biomater Sci Eng*. 2019;*5*:2793-2803.
30. Castilla-Casadiego DA, Pinzon-Herrera L, Perez-Perez M, Quiñonez-Colon B, Suleiman D, Almodovar J. Simultaneous characterization of physical, chemical, and thermal properties of polymeric multilayers using infrared spectroscopic ellipsometry. *Colloids Surf A*. 2018;*553*:155-168.
31. Haasters F, Prall WC, Anz C, et al. Morphological and immunocytochemical characteristics indicate the yield of early progenitors and represent a quality control for human mesenchymal stem cell culturing. *J Anat*. 2009;*214*:759-767.
32. Decher G, Hong JD, Schmitt J. Buildup of ultrathin multilayer films by a self-assembly process: III. Consecutively alternating adsorption of anionic and cationic polyelectrolytes on charged surfaces. *Thin Solid Films*. 1992;*210-211*:831-835.
33. Jha AK, Mathur A, Svedlund FL, Ye J, Yeghiazarians Y, Healy KE. Molecular weight and concentration of heparin in hyaluronic acid-based matrices modulates growth factor retention kinetics and stem cell fate. *J Control Release*. 2015;*209*:308-316.
34. Martino MM, Briquez PS, Ranga A, Lutolf MP, Hubbell JA. Heparin-binding domain of fibrin(ogen) binds growth factors and promotes tissue repair when incorporated within a synthetic matrix. *Proc Natl Acad Sci U S A*. 2013;*110*:4563-4568.
35. Sasisekharan R. Heparin and heparan sulfate: biosynthesis, structure and function. *Curr Opin Chem Biol*. 2000;*4*:626-631.
36. Brindley DA, Davie NL, Culme-Seymour EJ, Manson C, Smith DW, Rowley JA. Peak serum: implications of serum supply for cell therapy manufacturing. *Regen Med*. 2012;*7*:7-13.
37. Xuegang Y, Logan T, Ma T. Metabolism in human mesenchymal stromal cells: a missing link between hMSC biomanufacturing and therapy? *Front Immunol*. 2019;*10*:977.
38. Wang G, Kao K, Liu K, et al. Kynurenic acid, an IDO metabolite, controls TSG-6-mediated immunosuppression of human mesenchymal stem cells. *Cell Death Differ*. 2018;*25*:1209-1223.
39. Glenn JD, Whartenby KA. Mesenchymal stem cells: emerging mechanisms of immunomodulation and therapy. *World J Stem Cells*. 2014;*6*:526-539.
40. Cesarz Z, Tamama K. Spheroid culture of mesenchymal stem cells. *Stem Cells Int*. 2016;*2016*:1-11.
41. Burkin DJ, Jones C, Kimbro KS, Taylor MW, Barr BL, Gupta SL. Localization of the human indoleamine 2,3-dioxygenase (IDO) gene to the pericentromeric region of human chromosome 8. *Genomics*. 1993;*17*:262-263.
42. Takahashi H, Shibuya M. The vascular endothelial growth factor (VEGF)/VEGF receptor system and its role under physiological and pathological conditions. *Clin Sci*. 2005;*109*:227-241.
43. Andrae J, Gallini R, Betsholtz C. Role of platelet-derived growth factors in physiology and medicine. *Gene Dev*. 2008;*22*:1276-1312.
44. Wu J, Huang GT, He W, et al. Basic fibroblast growth factor enhances stemness of human stem cells from the apical papilla. *J Endod*. 2012;*38*:614-622.
45. Mihara M, Hashizume M, Yoshida H, Suzuki M, Shiina M. IL-6/IL-6 receptor system and its role in physiological and pathological conditions. *Clin Sci*. 2012;*122*:143-159.
46. Scheller J, Chalaris A. Schmidt-Arras; D.; rose-John, S. the pro- and anti-inflammatory properties of the cytokine interleukin-6. *Biochim Biophys Acta*. 1813;*2011*:878-888.
47. Jacques C, Gosset M, Berenbaum F, Gabay C. The role of IL-1 and IL-1Ra in joint inflammation and cartilage degradation. *Vitam Horm*. 2006;*74*:371-403.
48. Choi P, Reiser H. IL-4: role in disease and regulation of production. *Clin Exp Immunol*. 1998;*113*:317-319.
49. Beutler B, Cerami A. The biology of cachectin/TNF–a primary mediator of the host response. *Annu Rev Immunol*. 1989;*7*:625-655.
50. Fremd C, Schuetz F, Sohn C, Beckhove P, Domschke C. B cell-regulated immune responses in tumor models and cancer patients. *Onco Targets Ther*. 2013;*2*(7):e25443.
51. Melief SM, Zwaginga JJ, Fibbe WE, Roelofs H. Adipose tissue-derived multipotent stromal cells have a higher immunomodulatory capacity than their bone marrow-derived counterparts. *Stem Cells Transl Med*. 2013;*2*(6):455-463.
52. Klinker MW, Marklein RA, Lo Surdo JL, Wei C-H, Bauer SR. Morphological features of IFN-γ–stimulated mesenchymal stromal cells predict overall immunosuppressive capacity. *Proc Natl Acad Sci U S A*. 2017;*114*:E2598-E2607.
53. Marklein RA, Klinker MW, Drake KA, Polikowsky HG, Lessey-Morillon EC, Bauer SR. Morphological profiling using machine learning reveals emergent subpopulations of interferon-γ-stimulated mesenchymal stromal cells that predict immunosuppression. *Cytotherapy*. 2019;*21*:17-31.
54. Schwartz MA, Assoian RK. Integrins and cell proliferation: regulation of cyclin-dependent kinases via cytoplasmic signaling pathways. *J Cell Sci*. 2001;*114*(14):2553-2560.
55. Tsai CC, Chen YJ, Yew TL, et al. Hypoxia inhibits senescence and maintains mesenchymal stem cell properties through down-regulation of E2A-p21 by HIF-TWIST. *Blood Am J Hematol*. 2011;*117*(2):459-469.
56. Tang H, Xiang Y, Jiang X, et al. Dual expression of hTERT and VEGF prolongs life span and enhances angiogenic ability of aged BMSCs. *Biochem Biophys Res Commun*. 2013;*440*(4):502-508.
57. Ueyama H, Horibe T, Hinotsu S, et al. Chromosomal variability of human mesenchymal stem cells cultured under hypoxic conditions. *J Cell Mol Med*. 2012;*16*(1):72-82.
58. Gronthos S, Chen S, Wang CY, Robey PG, Shi S. Telomerase accelerates osteogenesis of bone marrow stromal stem cells by upregulation of CBFA1, osterix, and osteocalcin. *J Bone Miner Res*. 2003;*18*(4):716-722.
59. Pourgholaminejad A, Aghdami N, Baharvand H, Moazzeni SM. The effect of pro-inflammatory cytokines on immunophenotype, differentiation capacity and immunomodulatory functions of human mesenchymal stem cells. *Cytokine*. 2016;*85*:51-60.
60. Kim DS, Jang IK, Lee MW, et al. Enhanced immunosuppressive properties of human mesenchymal stem cells primed by interferon-γ. *EBioMedicine*. 2018;*28*:261-273.
61. Arumuggam N, Bhowmick NA, Rupasinghe HP. A review: phytochemicals targeting JAK/STAT signaling and IDO expression in cancer. *Phytother Res*. 2015;*29*:805-817.

62. Riopel M, Wang R. Collagen matrix support of pancreatic islet survival and function. *Front Biosci*. 2014;*19*:77-90.
63. Hind HG, Mcginn SM. Heparin content of adipose tissue. *Nature*. 1958;*182*:117-117.
64. Butterfield JH, Li C-Y. Bone marrow biopsies for the diagnosis of systemic Mastocytosis: is one biopsy sufficient? *Am J Clin Pathol*. 2004; *121*:264-267.
65. Martin C, Olmos E, Collignon ML, et al. Revisiting MSC expansion from critical quality attributes to critical culture process parameters. *Process Biochem*. 2017;*59*:231-243.
66. Avila MI, Rodriguez LG, Sánchez ML. Collagen: a review on its sources and potential cosmetic applications. *J Cosmet Dermatol*. 2018;*17*(1):20-26.
67. Onishi A, St Ange K, Dordick JS, Linhardt RJ. Heparin and anticoagulation. *Front Biosci*. 2016;*21*:1372-1392.
68. US Food and Drug Administration. Guidance for FDA reviewers and sponsors: content and review of chemistry, manufacturing, and control (CMC) information for human somatic cell therapy investigational new drug applications (INDs). Center for Biologics Evaluation and Research. 2008

SUPPORTING INFORMATION

Additional supporting information may be found online in the Supporting Information section at the end of this article.

How to cite this article: Cifuentes SJ, Priyadarshani P, Castilla-Casadiego DA, Mortensen LJ, Almodóvar J, Domenech M. Heparin/collagen surface coatings modulate the growth, secretome, and morphology of human mesenchymal stromal cell response to interferon-gamma. *J Biomed Mater Res*. 2020; 1–15. https://doi.org/10.1002/jbm.a.37085